DEVELOPMENT OF A NOVEL SOLID-STATE MODULATOR AND ITS APPLICATION IN HIGH-POWER KLYSTRONS[*]

X. Chen, C. Liu[†], F. Shang, L. Shang, W. Song, J. Pang, Z. He Z. Zhong
University of Science and Technology of China, Hefei, China

Abstract

This paper presents a highly integrated solid-state modulator designed to drive high-power klystrons in linear accelerators. The modulator employs a vertically integrated architecture in which the solid-state module array is directly combined with the high-voltage pulse transformer. This configuration eliminates long high-voltage cable connections, reduces parasitic inductance, and improves compactness and maintainability. The proposed modulator has been experimentally validated in high-power tests with an 80 MW S-band klystron at the Hefei Advanced Light Facility (HALF), achieving the required pulse waveform quality and stability. In addition, with limited modification, the same architecture can be adapted to higher repetition-rate applications such as the Super Tau-Charm Facility (STCF) injector, demonstrating its scalability for future large-scale accelerator facilities.

INTRODUCTION

High-power pulse modulators are essential for driving klystrons and other high-power microwave sources in linear accelerators [1]. The quality and stability of the modulator output directly affect beam performance and operational reliability in large-scale accelerator facilities. Owing to the lifetime limitations and maintenance burden of conventional thyratron-based systems, solid-state modulators based on insulated gate bipolar transistors (IGBTs) have become the mainstream solution in modern accelerator applications [2]. Their adoption in recent light-source facilities, including APS-U, MAX IV, and HEPS, has demonstrated the advantages of solid-state technology in reliability, controllability, and long-term operation [3–5].

Despite this progress, important engineering challenges remain in the practical deployment of high-power solid-state modulators. In conventional separated architectures, the power module array and the pulse transformer are often connected through long high-voltage transmission paths [6]. This arrangement increases parasitic inductance, which may aggravate voltage overshoot and transient waveform distortion. In addition, complex interconnections and enclosed modular layouts can reduce maintenance accessibility and prolong the mean time to repair, which is undesirable for accelerator facilities requiring high availability and efficient operation.

To overcome these challenges, this paper presents a novel solid-state modulator featuring a vertically integrated architecture that directly combines the power module array with the high-voltage pulse transformer. By eliminating long-distance high-voltage cabling and shortening the main current path, the proposed configuration reduces parasitic inductance and improves compactness and maintainability. The modulator has been experimentally validated in high-power operation with an 80 MW S-band klystron at the Hefei Advanced Light Facility (HALF). In addition, the adaptability of the same topology to higher repetition-rate applications, such as the STCF injector, is briefly discussed.

SYSTEM ARCHITECTURE AND DESIGN

To meet the stability, reliability, and maintainability requirements for driving high-power S-band klystrons, the proposed solid-state modulator adopts a highly integrated system architecture. As shown in Fig. 1, the system consists of four main parts: a primary high-voltage charging power supply, a modular solid-state power array, an integrated pulse transformer, and a central control and health management unit.

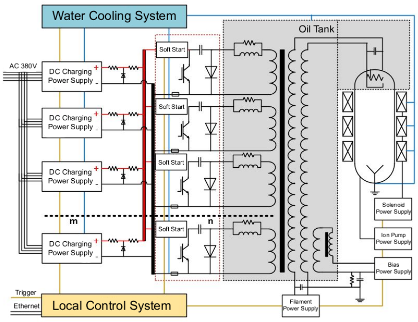

Figure 1: Block diagram of the proposed solid-state modulator system, including the primary charging supply, modular solid-state power array, integrated pulse transformer, and central control unit.

In operation, the primary charging supply provides a stable and adjustable DC input to the solid-state module array. When a synchronous trigger is applied, the active modules conduct simultaneously and generate a high-current primary pulse, which is delivered to the primary winding of the pulse transformer. The transformer then steps up the pulse to the required high-voltage level for driving the klystron cathode. Auxiliary power supplies are also included for the filament, focusing coils, and ion pump.

The proposed modulator features a vertically integrated architecture. Instead of using a conventional separated layout,

---

[*] This work was supported in part by the Fundamental Research Funds for the Central Universities (No. KY2310000050), in part by the Hefei Advanced Light Facility Project, and in part by the Super Tau-Charm Facility Key Technology Research Project.

[†] chaoliu@ustc.edu.cn

the solid-state module array is assembled as an independent enclosure and mounted directly on top of the pulse transformer oil tank, as shown in Fig. 2. This arrangement shortens the main pulse-current path and eliminates long external high-voltage cable connections between the module array and the transformer. As a result, distributed parasitic inductance is reduced, electrical layout is simplified, and maintenance access is improved. The compact layout also improves power density and facilitates installation and maintenance in large-scale accelerator facilities.

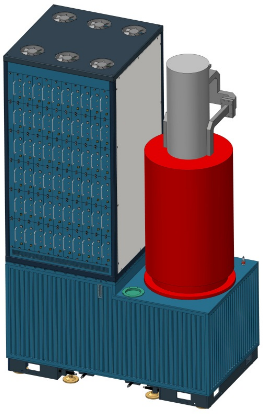

Figure 2: 3D mechanical model of the proposed vertically integrated modulator, with the solid-state module array mounted directly on the pulse transformer oil tank.

The main design parameters of the modulator for the 80 MW S-band klystron used in the HALF linac are summarized in Table 1. The system is designed to deliver an output pulse voltage above 415 kV and an output pulse current above 485 A, with a pulse stability better than 200 ppm (RMS) and a rise jitter below 10 ns. These specifications are set to satisfy the beam quality requirements of the injector system.

Table 1: Main Design Specifications of the Proposed Modulator for the 80 MW S-band Klystron in the HALF Linac

Parameter	**Specification**
Modulator Peak Power	≥ 200 MW
Output Pulse Voltage	≥ 415 kV
Output Pulse Current	≥ 485 A
HV pulse flattop width	≥ 1 µs
Pulse repetition rate	1 –10 Hz
Pulse Voltage Stability (RMS)	≤ 200 ppm
Output Pulse Rise Jitter (RMS)	≤ 10 ns

KEY DESIGN FEATURES

The proposed modulator adopts a vertically integrated architecture in which the solid-state module array is directly combined with the pulse transformer. Furthermore, particular attention is also given to the control and health management capability of the modulator, since reliable long-term operation requires effective supervision, diagnosis, and maintenance of the large parallel module array. In the present system, the central control unit coordinates the charging, triggering, protection, and diagnostic functions of the modulator, while continuously supervising the operating states of all power modules.

For the 120-module array, the control system continuously acquires key status information from each module, including fault state and thermal condition, thereby providing the basis for real-time status monitoring. Once an abnormal module is detected, the corresponding disconnect circuit is activated to isolate the faulty unit from pulse generation, while the remaining healthy modules continue operation under the redundant configuration. After isolation, the fault information is further mapped to the physical position of the module array, allowing rapid identification of the failed location and reducing maintenance time. Based on the real-time status distribution of the full module array, a quantitative health index is then calculated and presented to the operator as an intuitive indication of overall system condition and redundancy margin. The control and health-management interface is shown in Fig. 3. These functions improve the fault tolerance and maintainability of the integrated modulator and support reliable high-power klystron operation.

配电组件: 输入电压 ✓ 相序 ✓ 状态 开

高压电源: ON 982V

调制触发: τ 4us PRF 10Hz

偏磁电源: ON 4.75A

灯丝电源: ON 204V

固态调制器: ON 60 % 健康状态 60℃ 最高温度

速调管: 396.8kv 脉冲电压 358.6A 脉冲电流

聚焦线圈: 23.6A

水冷: 收集极水温 220V 速调管过温 ⚠ 流量 ⚠

钛泵电源: ON 3850V 5uA

聚焦电源: ON 220V 23.6A

脉冲变压器油箱: 脉冲电压 396.8kV 油温显示 26℃ 过温 ✓

外部信号: 辐射 ⚠ 联锁 ✓ 其他 ✓

阵列正面

✓	⚠	✓	✓	✓	✓	✓	✓	✓	✓
✓	⚠	✓	✓	✓	⚠	✓	✓	✓	✓
✓	⚠	✓	✓	✓	✓	✓	✓	✓	✓
✓	⚠	✓	✓	✓	⚠	✓	✓	✓	✓
✓	⚠	✓	✓	✓	✓	✓	✓	✓	✓
✓	⚠	✓	✓	✓	⚠	✓	✓	✓	✓

阵列背面

✓	⚠	✓	✓	✓	✓	✓	✓	✓	✓
✓	⚠	✓	✓	✓	⚠	✓	✓	✓	✓
✓	⚠	✓	✓	✓	✓	✓	✓	✓	✓
✓	⚠	✓	✓	✓	⚠	✓	✓	✓	✓
✓	⚠	✓	✓	✓	✓	✓	✓	✓	✓
✓	⚠	✓	✓	✓	⚠	✓	✓	✓	✓

操作建议: ✓ 运行

88 % 健康指数

Figure 3: Control and health-management interface of the modulator, showing real-time module status, fault location, and the calculated health index of the module array.

To further support pulse-to-pulse reproducibility, the modulator is supplied by a high-precision programmable SiC DC charging power supply, and a synchronous isolation mechanism is introduced between the charging stage and the modulator array. By electrically isolating the primary supply from the high-current discharge process, the disturbance imposed on the voltage regulation loop is suppressed, providing the electrical basis for the stable flattop performance demonstrated in the high-power tests.

EXPERIMENTAL RESULTS AND APPLICATIONS

To verify the engineering performance of the proposed modulator, high-power tests was carried out at the HALF linac test facility. As shown in Fig. 4, multiple solid-state modulator units were deployed in parallel for klystron conditioning, serving as the high-power test platform at the HALF linac.

The output high-voltage pulse was measured through a high-voltage divider, and the flattop stability was evaluated using a differential amplifier together with a digital oscilloscope. A representative oscilloscope waveform used in the stability measurement is shown in Fig. 5, where the differential flattop-fluctuation signal, the timing trigger, and the divided pulse-voltage waveform are simultaneously recorded.

Figure 4: High-power test platform of the proposed solid-state modulator at the HALF linac facility.

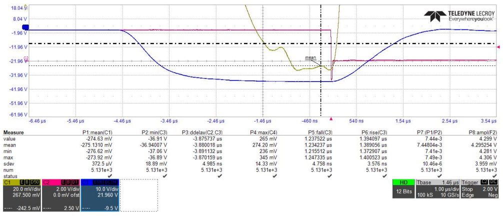

Measure	P1:mean(C1)	P2:min(C3)	P3:ddelay(C2,C3)	P4:max(C4)	P5:fall(C3)	P6:rise(C3)	P7:(P1/P2)	P8:ampl(F2)
value	-274.63 mV	-36.91 V	-3.875737 µs	265 mV	1.237522 µs	1.394097 µs	7.44e-3	4.299 V
mean	-275.1310 mV	-36.94007 V	-3.880018 µs	274.20 mV	1.234237 µs	1.389056 µs	7.44804e-3	4.295254 V
min	-276.62 mV	-37.06 V	-3.891132 µs	236 mV	1.215512 µs	1.372907 µs	7.41e-3	4.281 V
max	-273.92 mV	-36.89 V	-3.870159 µs	345 mV	1.247335 µs	1.400523 µs	7.49e-3	4.306 V
sdev	372.5 µV	18.89 mV	4.985 ns	14.33 mV	4.758 ns	3.576 ns	10.46e-6	3.959 mV
num	5.131e+3	5.131e+3	5.131e+3	5.131e+3	5.131e+3	5.131e+3	5.131e+3	5.131e+3
status	✓	✓	✓	✓	✓	✓	✓	✓

C1	C2	C3
20.0 mV/div	2.00 V/div	10.0 V/div
267.500 mV	0.0 mV ofst	21.960 V
-242.5 mV	2.50 V	-9.5 V

Figure 5: Representative oscilloscope traces used for pulse-to-pulse stability measurement, showing the differential flattop-fluctuation signal, the timing trigger, and the divided pulse-voltage waveform.

Under the rated operating conditions of 390 kV and 10 Hz, the modulator generated a stable high-voltage pulse with a well-defined flattop and no significant overshoot. To evaluate pulse-to-pulse reproducibility, continuous measurements were performed over 5,000 pulses. The statistical result, shown in Fig. 6, indicates a pulse amplitude stability of 136 ppm (RMS) at the flattop. This value is well below the design limit of 200 ppm and confirms that the proposed modulator can satisfy the stability requirement for high-power klystron operation in the HALF injector. The other key performance parameters, including output pulse voltage, output pulse current, flattop width, repetition rate, and pulse rise jitter, were also verified to satisfy the design requirements listed in Table 1.

Furthermore, the same modulator topology is suitable for higher repetition-rate systems. One representative case is the STCF injector, which requires a large-scale pulsed power system operating at up to 90 Hz to support the swap-out injection scheme [7].

For this operating regime, the main adaptation is associated with average-power handling and thermal management rather than a fundamental change of the architecture. On the basis of the validated integrated topology, the upgrade mainly involves enhanced cooling for the solid-state module array and high-voltage components. This engineering path preserves the structural advantages of the proposed modulator while extending its applicability to more demanding high-repetition-rate accelerator facilities.

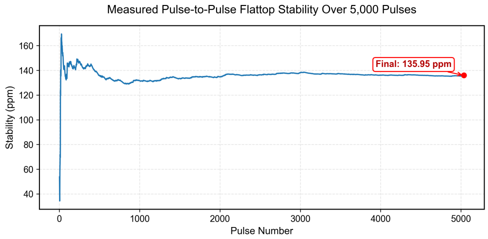

Figure 6: Measured pulse-to-pulse flattop stability of the modulator over 5,000 consecutive pulses at rated operating conditions.

CONCLUSION

This paper has presented a highly integrated solid-state modulator for high-power klystron applications, with particular emphasis on its vertically integrated architecture. The proposed system also incorporates control and health management functions for real-time module monitoring, fault isolation, fault localization, and quantitative condition evaluation, thereby improving maintainability and operational availability in accelerator service.

High-power tests at the HALF linac has demonstrated stable operation with an 80 MW S-band klystron, including a measured pulse-to-pulse flattop stability of 136 ppm (RMS), which satisfies the design requirement. The same topology can be extended to higher repetition-rate applications such as the STCF injector with limited engineering adaptation, mainly in thermal management. These results indicate that the proposed modulator architecture provides a practical and scalable solution for future accelerator pulsed power systems.

REFERENCES

[1] G. Caryotakis, “High power klystrons: Theory and practice at the Stanford Linear Accelerator Center Part 1, Theory and design”, Menlo Park, CA, USA, Rep. SLAC-PUB-10620, Aug. 2004. doi:10.2172/839705

[2] R. L. Cassel, G. C. Pappas, M. N. Nguyen, and J. E. DeLamare, “A Solid State Induction Modulator for SLAC NLC”, in *Proc. PAC’99*, New York, NY, USA, Mar. 1999, paper TUP9, pp. 1494–1496. doi:10.1109/PAC.1999.794145

[3] T. J. Russell and A. Cours, “Klystron Modulator Operation and Upgrades for the APS Linac”, in *Proc. PAC’95*, Dallas, TX, USA, May 1995, paper TAQ16, pp. 1559–1560. doi:10.1109/PAC.1995.505285

[4] D. Olsson, F. Curbis, E. Mansten, S. Thorin, and S. Werin, “Transverse RF Deflecting Structures for the MAX IV LINAC”, in *Proc. IPAC’18*, Vancouver, Canada, Apr.-May 2018, pp. 3684–3687. doi:10.18429/JACoW-IPAC2018-THPAL027

[5] C. Meng *et al.*, “Beam commissioning of the HEPS Linac”, in *Proc. IPAC’23*, Venice, Italy, May 2023, pp. 2023–2026. doi:10.18429/JACoW-IPAC2023-TUPL126

[6] S. Choroba, “Design and Status of the XFEL RF System”, in *Proc. PAC’07*, Albuquerque, NM, USA, Jun. 2007, paper TUXC03, pp. 841–845.

[7] X.-C. Ai *et al.*, “Conceptual design report of the Super Tau-Charm Facility: the accelerator”, *Nucl. Sci. Tech.*, vol. 36, no. 12, p. 242, 2025. doi:10.1007/s41365-025-01833-x